ISSN 0030-400X, Optics and Spectroscopy, 2012, Vol. 112, No. 2, pp. 223–232. © Pleiades Publishing, Ltd., 2012.
Original Russian Text © O.K. Bazyl', V.Ya. Artyukhov, G.V. Maier, G.B. Tolstorozhev, T.F. Raichenok, I.V. Skornyakov, O.I. Shadyro, V.L. Sorokin, G.A. Ksendzova, 2012, published in Optika i Spektroskopiya, 2012, Vol. 112, No. 2, pp. 248–257.

CONDENSED-MATTER SPECTROSCOPY

Electronic Structure and Spectroscopic Properties of Anti-HIV Active Aminophenols

O. K. Bazyl'[a], V. Ya. Artyukhov[a], G. V. Maier[a], G. B. Tolstorozhev[b], T. F. Raichenok[b], I. V. Skornyakov[b], O. I. Shadyro[c], V. L. Sorokin[c], and G. A. Ksendzova[c]

[a] *Tomsk State University, Tomsk, 634050 Russia*

[b] *B.I. Stepanov Institute of Physics, National Academy of Sciences of Belarus, Minsk, 220072 Belarus*

[c] *Belarusian State University, Minsk, 220050 Belarus*

Received July 18, 2011

Abstract—We have measured the absorption and fluorescence spectra and fluorescence quantum yields of sulphone-containing anti-HIV active *o*-aminophenol molecules in an inert solvent, hexane, and in a polar solvent, acetonitrile. We have studied IR Fourier-transform spectra and examined structural features of *o*-aminophenols with different substituents in solutions and crystals. Functional groups of molecules that are involved in the formation of hydrogen bonds have been revealed. Proton acceptor properties of *o*-aminophenol molecules have been theoretically evaluated using the method of molecular electrostatic potential. Using quantum chemistry methods, we have calculated and interpreted absorption and fluorescence spectra of *o*-aminophenols. Calculation data are compared with experimental results. We have determined the main channels and mechanisms of photophysical relaxation processes in *o*-aminophenols.

DOI: 10.1134/S0030400X12010031

INTRODUCTION

The introduction into medical practice of drugs that suppress HIV infection in humans is a socially important problem [1].

At present, it seems necessary to continue the search for new compounds with a high level of anti-HIV activity. Derivatives of aminophenol, which possess high antioxidant properties [2], can be considered such compounds. Recently, sulphone-containing derivatives of aminophenol that are capable of suppressing HIV infection in cell culture have been synthesized [3].

Full-scale application of aminophenol in HIV therapy is possible provided that the main factors that affect the pharmacotherapeutic activity of these compounds are known. A systematic investigation of the electronic structure of molecules and an elucidation of the relationships between the optical properties and pharmacological action of aminophenol are necessary.

The importance of complex quantum-chemical and spectroscopic investigations of aminophenols is indisputable. This implies a detailed study of the properties of isolated molecules, determination of particular features of the formation of intramolecular and intermolecular hydrogen bonds, and clarification of the role played by the medium in the manifestation of the pharmacological activity of *o*-aminophenols [4–7].

This paper presents our experimental and theoretical investigations of the electronic structure, proton acceptor and spectral–luminescent properties, and mechanisms of photophysical processes in sulphone-containing aminophenol derivatives.

MATERIALS AND METHODS

As objects of study, we used N-(2-hydroxy-3,5-di-*tert*-butyl)-4-methylbenzenesulphonamide (AP I), N-(2-methoxy-3,5-di-*tert*-butylphenyl)-4-methylbenzenesulphonamide (AP II), N-(2-hydroxy-3,5-di-*tert*-butylphenyl)-4-methanesulphonamide (AP III), N-(2-hydroxy-3,5-di-*tert*-butylphenyl)-4-benzenesulphonamide (AP IV), N-(2-hydroxy-3,5-di-isopropylphenyl)-4-methylbenzenesulphonamide (AP V), N-(2-hydroxy-3,5-di-isopropylphenyl)-4-benzenesulphonamide (AP VI), N-(2-hydroxy-3,5-di-isopropylphenyl)methanesulphonamide (AP VII), and N-(2-methoxy-3,5-di-*tert*-butylphenyl)methanesulphonamide (AP VIII).

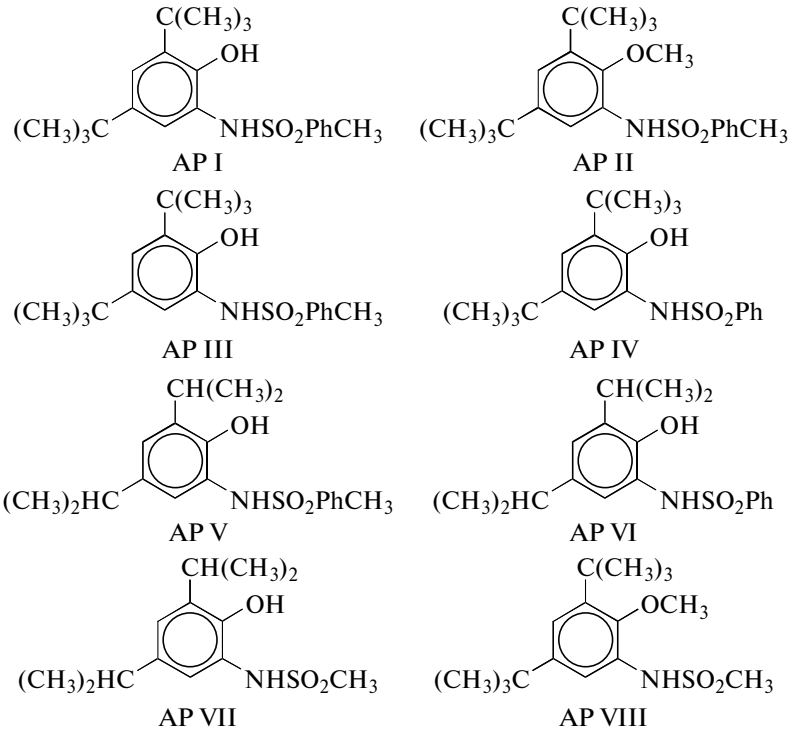

Hereinafter, the phenyl ring of the *o*-aminophenol fragment will be denoted as Ph1, and the phenyl ring of the in the sulphone substituent will be denoted as Ph2.

Aminophenol compounds were synthesized according to techniques described in [7]. The correctness of the chemical structure of synthesized aminophenol derivatives was confirmed by data of mass-spectrometry, NMR, and elemental analysis.

The IR spectra of aminophenol crystals were measured with a resolution of 2 cm^{-1} and averaging over 256 scans on a Nexus IR Fourier-transform spectrometer equipped with the OMNIC software. The measurements were performed using an IR microscope, in which the IR radiation was incident onto an area of 5 μm^2 on the crystal surface of the sample at an almost normal angle, was transmitted through the crystal, was reflected from a metalized substrate, and was transmitted once more through the bulk of the crystallized sample.

The electronic absorption spectra of solutions of aminophenols were measured on a CARY-500 spectrophotometer, and the spectra and quantum yields (γ_{exc}) of fluorescence were measured on CM-2203 and HORIBA Jobin Yvon spectrofluorimeters.

Quantum-chemical calculations of the electronic structure of aminophenol molecules were performed by the method of intermediate neglect of differential overlap (INDO) with spectroscopic parameterization [8]. The method was applied using the software package from [9]. The rate constants of photophysical processes of deactivation of electronically excited states of molecules, which are necessary for determining relaxation channels of the electronic excitation energy, were calculated, and fluorescence quantum yields were found. The methods for estimation rate constants of nonradiative processes were described in [8].

The proton acceptor properties of molecules in the ground and first singlet excited states were calculated by the method of molecular electrostatic potential (MEP) [10] using the wave functions obtained by the INDO method. MEP calculations were performed using the deorthogonalized basis set from [8].

In calculations of the electronic structure of aminophenol molecules, the choice of the spatial conformation is important, since aminophenol derivatives have several single bonds, and the possibility of rotation of fragments of the molecule is admitted. In addition, the mutual spatial arrangement of individual fragments of the molecule plays an important role in the estimation of proton acceptor properties of molecules, since this substantially affects the magnitude of the MEP. The geometry of aminophenol molecules was optimized based on the density functional theory using the ADF software package [12]. The IR spectra of aminophenol molecules yield useful information for choosing the most probable conformer of the molecule [4–7]. An analysis of these spectra showed that all *o*-aminophenol molecules that contain hydroxyl group are characterized by the presence of hydrogen bonds of the O–H...N type [4, 5].

RESULTS AND DISCUSSION

IR spectra aminophenols. The study of the IR spectra of 10^{-3} M CCl_4 solutions of all eight sulphone-containing aminophenols has shown that the absorption bands with the frequencies of their maxima ν_{max} = 3638, 3425, and 3250 cm^{-1} are caused by stretching vibrations of free and associated OH groups, while bands with ν_{max} = 3510 and 3360 cm^{-1} occur due to free and coupled vibrations N–H [7, 14].

The occurrence of the absorption band of coupled vibrations O–H with ν_{max} = 3425 cm^{-1} in the IR spectra of aminophenol molecules is related to the formation of intramolecular hydrogen bonds of the O–H...N type [7, 14]. The occurrence of the band of coupled vibrations of NH groups with ν_{max} = 3360 cm^{-1} in the IR spectra of aminophenol solutions was interpreted by the formation of intramolecular hydrogen bonds N–H...O=S in aminophenol molecules [7, 14].

It is undoubtedly interesting to study in detail the behavior of the OH, NH, and SO_2 functional groups in aminophenol molecules upon passage from the solution to the crystal and to determine spectral attributes of the anti-HIV activity of these compounds using methods of IR Fourier-transform spectroscopy.

Figure 1 presents IR spectra of the AP I–AP V crystals in the spectral range 3700–2700 cm^{-1}. This range contains absorption bands of stretching vibrations of the OH and NH groups, which are capable of participating in intramolecular and intermolecular interactions [4–7], as well as absorption bands of stretching vibrations of C–H bonds of the aromatic ring, methyl, isopropyl, and *tert*-butyl groups. Bands of stretching vibrations of C–H bonds lie in the range 3000–2700 cm^{-1} and are characteristic of all aminophenol compounds. In investigation of hydrogen bonds, they were used as "internal standards" to which IR spectra were normalized.

Experiments with cell cultures showed that compounds AP I and AP V are active in suppressing HIV infection, whereas compounds AP II, AP III, and AP IV are inactive [3].

It follows from Fig. 1 that OH and NH groups of aminophenol molecules participate in intermolecular interactions. This is evidenced by the occurrence of absorption bands of coupled vibrations of OH and NH groups in IR spectra of aminophenols.

The spectrum of the crystal of anti-HIV active AP I exhibits bands of O–H coupled vibrations with ν_{max} = 3552, 3285, and 3236 cm^{-1} (curve *1*). In IR spectra of AP I solutions, free OH groups are characterized by the band with ν_{max} = 3638 cm^{-1} [6, 7]. In the IR spectrum of the solution of AP I in CCl_4, the band of coupled O–H vibrations with ν_{max} = 3425 cm^{-1} was also observed, which is a consequence of the participation of OH groups in the formation of intramolecular hydrogen bonds of the O–H...N type [7, 14]. Upon passage from the solution to the crystal, instead of this absorption band, the IR spectrum of the AP I crystal shows the band of O–H vibrations with ν_{max} = 3552 cm^{-1} (curve *1*). The shift of the absorption maximum of coupled vibrations of OH groups in the IR spectrum of the crystal to the high-frequency range by 127 cm^{-1} is caused by the fact that, in the crystal, intramolecular hydrogen bonds of the O–H…N type, which exist in the solution, are broken and intermolecular hydrogen bonds with the participation of OH groups are formed instead [7].

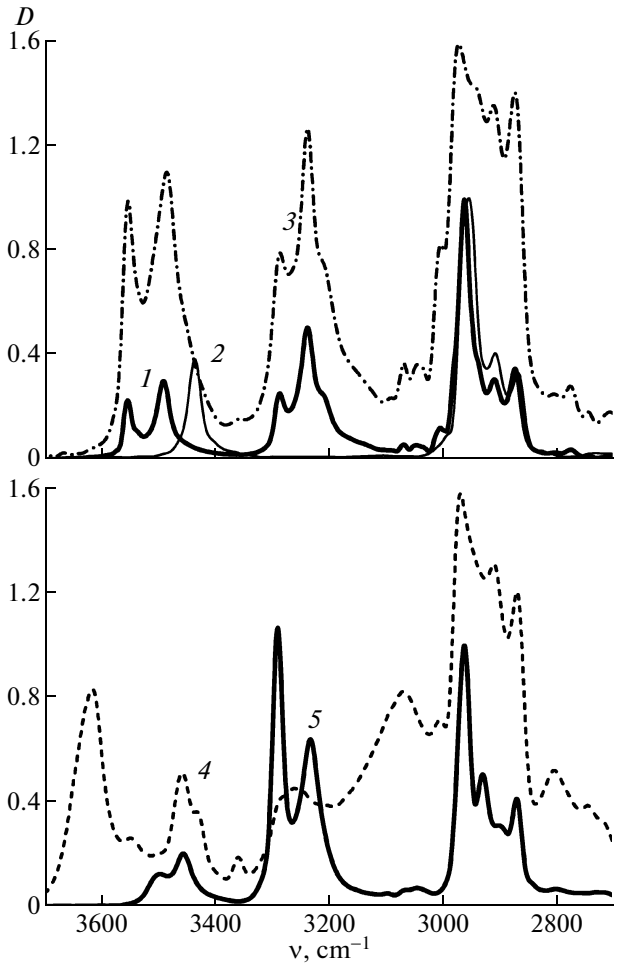

Fig. 1. IR spectra of crystals (*1*) AP I, (*2*) AP II, (*3*) AP III, (*4*) AP IV, and (*5*) AP V in the range of stretching vibrations of the OH and NH groups.

In the IR spectra of solutions of all the sulphone-containing aminophenols, free NH groups are characterized by an absorption band with ν_{max} = 3510 cm^{-1} [6, 7]. In the spectrum of the crystal of anti-HIV active AP I, the band of coupled N–H vibrations is shifted toward the low-frequency range compared to the absorption of free NH groups and has ν_{max} = 3484 cm^{-1} (curve *1*). Comparison of the IR spectrum of the crystal with the IR spectrum of the solution of AP I in CCl_4

shows that, in the spectrum of the crystal, the band of coupled N–H vibrations ($\nu_{max} = 3484$ cm^{-1}) is shifted with respect to its position in the spectrum of the solution ($\nu_{max} = 3360$ cm^{-1}) toward the high-frequency range by 126 cm^{-1}. This means that, in the crystal, there are no conditions for preserving intramolecular hydrogen bonds of the N–H...O=S type, which exist in the solution, and amino groups participate in the formation of intermolecular hydrogen bonds of the N–H...O type.

Since molecules of the crystal of inactive AP II do not contain OH groups, only the band of coupled N–H vibrations with the maximum at $\nu_{max} = 3434$ cm^{-1} is observed in its spectrum (curve *2*).

In the spectrum of the crystal of inactive AP III (curve *3*), the absorption band of N–H vibrations with $\nu_{max} = 3484$ cm^{-1} is observed, as well as the bands of O–H vibrations with $\nu_{max} = 3552$, 3285, 3236, and 2938 cm^{-1}. An increase in the absorption in the range of vibrations of C–H bonds at 2938 cm^{-1} in the IR spectrum of the compound AP III is caused by vibrations of OH groups, which participate in the formation of intermolecular hydrogen bonds. There are no hydrogen bonds of this type in crystals of the anti-HIV active compound AP I.

The range of O–H vibrations in the IR spectrum of the crystal of inactive AP IV differs even more from this range in the spectrum of the crystal of AP I. The spectrum of the crystal of AP IV (curve *4*) contains an intense absorption band of vibrations of free OH groups with $\nu_{max} = 3614$ cm^{-1}, as well as broad bands of coupled vibrations of OH groups with $\nu_{max} = 3259$, 3067, and 2940 cm^{-1}.

In the IR spectrum of the crystal of anti-HIV active compound AP V (curve *5*), the bands of coupled O–H vibrations with $\nu_{max} = 3495$, 3288, and 3231 cm^{-1} are observed, and the band of coupled N–H vibrations is shifted to $\nu_{max} = 3454$ cm^{-1}.

Collation of the IR spectra of anti-HIV active compounds AP I and AP V shows that, in the range of O–H and N–H stretching vibrations, these two compounds have close spectral characteristics, which considerably differ from those of the IR spectra of inactive compounds AP II, AP III, and AP IV.

In the IR spectra of the AP I and AP V crystals, the band maximum of coupled O–H vibrations is shifted toward the low-frequency range by 85 and 119 cm^{-1}, respectively, with respect to ν_{max} of the absorption band of free OH groups. The IR spectra of the crystals of the anti-HIV active compounds also exhibit two closely located bands of coupled O–H vibrations, with their maxima being located at $\nu_{max} = 3285$ and 3236 cm^{-1} (AP I) and at $\nu_{max} = 3288$ and 3231 cm^{-1} (AP V). In the IR spectra of the crystals of anti-HIV active compounds, N–H vibrations also experience a low-frequency shift of their ν_{max}, namely, by 26 cm^{-1} for AP I and by 72 cm^{-1} for AP V.

Therefore, in crystals of anti-HIV active aminophenols, intermolecular interactions of the same type occur, which involve the participation of hydroxyl and amino groups of these compounds. The hydrogen bonds of the following types are most likely to occur: O–H…O, N–H…O, and O–H…N.

Electron density and proton acceptor properties of aminophenols. In order to determine functional groups with which OH and NH groups interact upon formation of intermolecular hydrogen bonds in crystals, we considered the distribution of effective charges in the molecule and estimated the proton acceptor properties of molecules in the ground and first singlet excited states by the MEP method.

Table 1 presents electron density distributions on fragments of the examined aminophenols in the ground and first excited electronic states. In the ground state of all the aminophenol derivatives under study, aromatic phenyl ring Ph1 shows donor properties. In all the derivatives that contain phenyl ring Ph2 in the substituent of the amino group NH, this ring also is the electron-density donor. *Tert*-butyl (or isopropyl) substituents and methyl group in phenyl Ph2 exhibit donor properties, whereas, in the majority of considered aminophenol derivatives, the NH and SO_2 fragments are acceptors.

Our calculations showed that the donor–acceptor properties of phenyl ring Ph1 in aminophenol molecules noticeably depend on the presence or absence of other substituents in the molecule. Thus, the absence of fragment Ph2 in AP III, AP VII, and AP VIII reduces the donor capabilities of phenyl Ph1 and increases the acceptor capabilities of NH groups (AP I and AP III; Table 1). The absence of fragment Ph2 in AP III, AP VII, and AP VIII has an especially strong effect on the properties of the sulphone group: in the absence of Ph2, the SO_2 fragment becomes an electron-density donor, whereas, in the presence of Ph2, it displays acceptor properties (AP I and AP III; AP II and AP VIII; Table 1). The occurrence of fragment Ph2 also affects the properties hydroxy- and methoxy-derivatives. In *o*-aminophenols with the Ph2 fragment, changes that are introduced upon replacement of the OH group by the methoxy group are the most significant for fragment NH. In the absence of Ph2 (AP III and AP VIII; Table 1), the methoxy group noticeably changes the donor properties of phenyl Ph1 and *tert*-butyl substituents.

Replacement of *tert*-butyl substituents by isopropyl ones (AP III and AP VII; AP IV and AP VI; Table 1) has an effect not only on ring Ph1, in which various replacements take place, but also on spatially distant fragments, such as the NH group and phenyl Ph2. Replacement of hydroxyl OH groups by methoxy groups (AP III and AP V) changes the properties of isopropyl groups, increasing their donating properties

Table 1. Electron density distribution on fragments of aminophenol molecules in the ground and excited states

Compound	Effective charge of fragment (e)							
	State	Ph1	Ph2	$C(CH_3)_3$ or $CH(CH_3)_2$	OH or OCH_3	NH	SO_2	CH_3
AP I	S_0	0.231	0.118	0.078	−0.193	−0.145	−0.156	0.053
	$S_1(\pi\pi^*)$	0.226	0.013	0.141	−0.077	−0.172	−0.181	0.074
AP II	S_0	0.223	0.125	0.061	−0.133	−0.171	−0.158	0.053
	$S_1(\pi\pi^*)$	0.161	0.009	0.138	−0.013	−0.164	−0.179	0.048
AP III	S_0	0.099	–	0.095	−0.120	−0.200	0.078	0.048
	$S_1(\pi\pi^*)$	−0.107	–	0.133	−0.059	−0.122	0.100	0.055
AP IV	S_0	0.231	0.166	0.079	−0.144	−0.172	−0.155	–
	$S_1(\pi\pi^*)$	0.229	0.059	0.136	−0.077	−0.166	−0.181	–
AP V	S_0	0.242	0.125	0.071	−0.158	−0.178	−0.155	0.053
	$S_1(\pi\pi^*)$	0.290	0.002	0.119	−0.092	−0.180	−0.190	0.051
AP VI	S_0	0.262	0.169	0.029	−0.151	−0.204	−0.105	–
	$S_1(\pi\pi^*)$	0.270	0.050	0.112	−0.082	−0.202	−0.148	–
AP VII	S_0	0.088	–	0.115	−0.124	−0.171	0.038	0.054
	$S_1(\pi\pi^*)$	−0.093	–	0.141	−0.047	−0.102	0.049	0.052
AP VIII	S_0	0.113	–	0.139	−0.180	−0.186	0.069	0.045
	$S_1(\pi\pi^*)$	−0.065	–	0.118	−0.027	−0.101	0.067	0.008

as compared to *tert*-butyl groups. An interesting effect is produced by the CH_3 group introduced in the *para*-position of phenyl Ph2. In the absence of the methyl group, ring Ph1 and *tert*-butyl substituents do not change their properties in different compounds (AP I and AP IV; AP V and AP VI; Table 1), whereas the properties of the NH and OH groups and Ph2 change. Replacement of *tert*-butyl substituents by isopropyl ones in the absence of the CH_3 group leads to changes in the donor–acceptor properties of these fragments and to changes in the properties of fragment Ph1 and the SO_2 group.

Upon excitation to the S_1 state, all fragments of aminophenols, except for phenyl Ph1, retain their donor–acceptor properties. In the excited state and in the absence of phenyl Ph1, fragment Ph2 becomes an acceptor of the electron density.

Therefore, the distribution of the electron density among fragments of aminophenols (Table 1) indicate that the formation of a hydrogen bond between the proton and the oxygen atom of the hydroxyl group OH, the oxygen atoms of the SO_2 group, and the nitrogen atom N of the amino group NH is most probable.

Table 2 presents calculated minima of the MEP for isolated molecules of all the aminophenol derivatives. It follows from these calculations that, for AP I–AP VIII, there are three characteristic ranges of interaction of the proton with the oxygen atom of the hydroxyl group OH and the oxygen atoms of the SO_2 group. The strongest interaction should be expected between the proton and the oxygen atoms of the SO_2 group. The absence of a minimum of the MEP near the nitrogen atom is explained by the fact that its negative charge is screened by positive charges of sulfur and nearby hydrogen atoms.

Despite the fact that, on the whole, OH and NH groups display donor properties (Table 1), their ability to form hydrogen bonds is determined by a high effective charge of the hydrogen atom, which is equal to 0.19 e for OH and to 0.14 e for NH and which is an almost an order of magnitude higher than the effective charges of hydrogens of aromatic cycles and methyl groups. This confirms the activity of hydrogens of the OH and NH groups in the formation of hydrogen bonds. At the same time, a high proton acceptor ability of oxygens of the SO_2 group (Table 2) makes it possible to assume that intermolecular hydrogen bonds are most likely formed between protons of OH or NH groups and oxygens of sulphone groups.

Absorption spectra. Figure 2 shows absorption spectra of AP I–AP VIII.

In the absorption spectra of substituted *o*-aminophenols, the following three ranges can be singled out: the long-wavelength range ($\lambda > 260$ nm), the intermediate range (from $\lambda = 260$ to 225 nm), and the short-wavelength range ($\lambda < 225$ nm). Comparison of these spectra shows that the greatest changes in the position and intensity of the absorption bands are observed upon replacement of the hydroxyl group by the methoxy group (AP I and AP II, as well as AP III and AP VIII; Fig. 2, curves *1–3*, *8*; Table 3). In this

Table 2. Minima of MEP (U) of aminophenol derivatives

Compound	U, kJ/mol					
	O(OH or OCH_3-group)		$O_1(SO_2$-group)		$O_2(SO_2$-group)	
	S_0	S_1	S_0	S_1	S_0	S_1
AP I	−296	−198	−936	−946	−904	−926
AP II	−285	−140	−932	−939	−903	−926
AP III	−285	−159	−919	−952	−888	−952
AP IV	−293	−195	−930	−941	−898	−921
AP V	−338	−242	−938	−944	−884	−905
AP VI	−340	−227	−948	−957	−872	−896
AP VII	−333	−257	−873	−835	−860	−836
AP VIII	−297	−248	−800	−779	−785	−747

case, the intensities of bands in the intermediate range decrease and the long-wavelength band somewhat narrows.

In the absence of the methyl group (AP IV and AP VI), the absorption bands in the intermediate range of the spectrum shift toward the short-wavelength range (Fig. 2, curves *4*, *6*). The presence of fragment Ph2 in aminophenol molecules leads only to a long-wavelength shift of these absorption bands by 1–5 nm (AP V and AP VII; Fig. 2, curves *5* and *7*; Table 3).

According to quantum-chemical calculations, in examined compounds AP I–AP VIII, electronic transitions with participation of phenyl Ph1 make the main contribution to the formation of the intensity in all the ranges of the absorption spectrum. We can single out three absorption bands the intensities and maximum positions of which are close to experiment (Table 3).

It should be noted that the long-wavelength band in the absorption spectrum of AP I–AP VIII is formed by two transitions, $S_0 \rightarrow S_1$ and $S_0 \rightarrow S_2$. The most intense

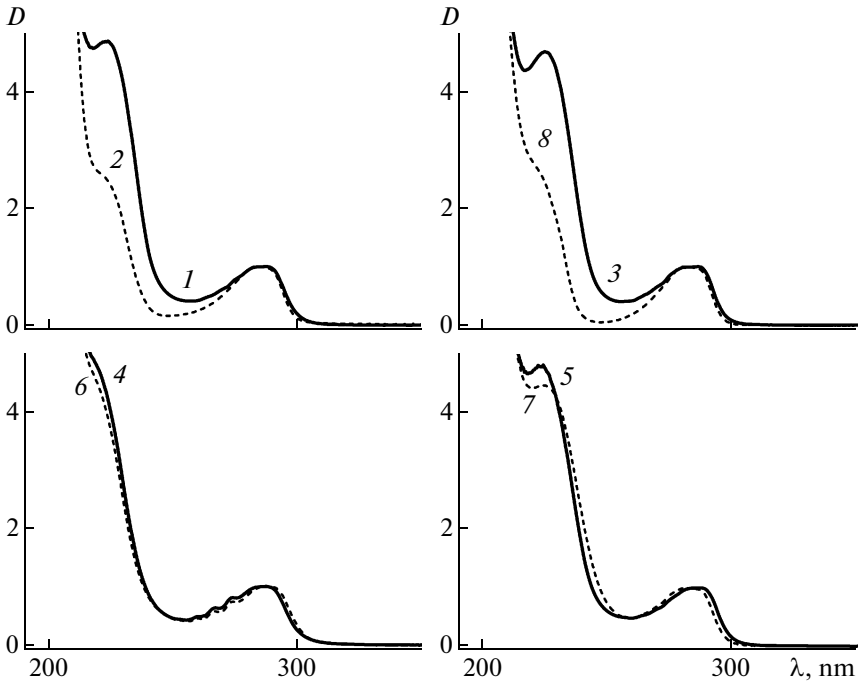

Fig. 2. Electronic absorption spectra of solutions of (*1*) AP I, (*2*) AP II, (*3*) AP III, (*4*) AP IV, (*5*) AP V, (*6*) AP VI, (*7*) AP VII, and (*8*) AP VIII in (*1*, *2*, *4*, and *6*) hexane and (*3*, *5*, *7*, *8*) acetonitrile.

Table 3. Calculated and experimental absorption spectra of AP I–AP VIII

Calculation			Experiment					
			hexane			acetonitrile		
S_i	E_i, cm^{-1}	f	E, cm^{-1}	λ_{max}, nm	ε, L/mol cm	E, cm^{-1}	λ_{max}, nm	ε, L/mol cm
				AP I				
S_1	34790	0.043	34780	287.5	4000	35150	284.5	4000
S_2	37820	0.004						
S_8	44580	0.692	44840	223.0	19400	44640	224.0	18500
S_9	45280	0.268						
				AP II				
S_1	34460	0.053	35270	283.5	–*	35340	283.0	4300
S_2	37760	0.004						
S_7	43520	0.104	44840	223.0	–*	45045	222.0	12000
S_8	43720	0.455						
S_{10}	45170	0.323						
				AP III				
S_1	33730	0.038	34840	287.0	–*	34965	286.0	3000
S_2	39460	0.007						
S_7	44390	0.460	44740	223.5	–*	44440	225.0	14000
S_8	45610	0.227						
				AP IV				
S_1	34740	0.045	34960	286.0	3900	3900	286.0	4000
S_2	38400	0.001						
S_8	44410	0.095	45870	218.0	19000	19000	218.0	19000
S_9	45410	0.319						
S_{10}	45760	0.735						
				AP V				
S_1	34690	0.052	34600	289.0	4000	34900	286.5	3900
S_2	37750	0.003						
S_8	44210	0.909	44840	223.0	18700	44840	222.0	18700
S_9	44930	0.148						
				AP VI				
S_1	34830	0.057	34600	289.0	3750	34960	286.0	3750
S_2	38410	0.001						
S_8	44470	0.765	44840	220.0	16500	44840	220.0	17500
S_9	46000	0.299						
				AP VII				
S_1	33690	0.035	35520	281.5	–*	35590	281.0	2800
S_2	39110	0.019						
S_7	44900	0.139	44440	225.0	–*	4444	225.0	12500
S_8	45370	0.698						
				AP VIII				
S_1	34020	0.029	35590	281.0	–*	35590	281.0	3200
S_2	39660	0.086						
S_6	43725	0.321	45045	222.0	–*	45045	222.0	8500
S_9	46480	0.432						

* Insufficient solubility.

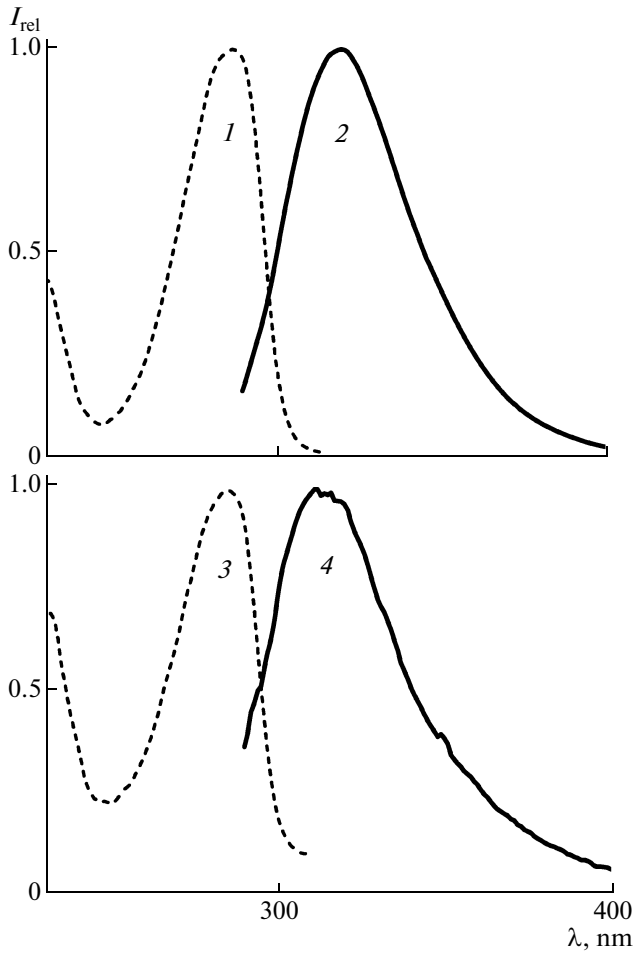

Fig. 3. (*1*, *3*) Fluorescence excitation and (*2*, *4*) fluorescence excitation spectra of solutions of (*1*, *2*) AP II and (*3*, *4*) AP VIII in hexane.

of them is the transition $S_0 \rightarrow S_1(\pi\pi^*)$, which is formed by configurations of molecular orbitals (MOs) localized on the aromatic ring of Ph1 with the participation of atomic orbitals (AOs) of the oxygen atom of the hydroxyl group and the nitrogen atom.

The intensity of the intermediate absorption band of molecules AP III, AP VII, and AP VIII is formed by two electronic transitions, which are formed by configurations of MOs of the Ph1 ring without participation of AOs of the oxygen atom of the OH group and nitrogen. In addition, the intermediate absorption band is contributed by configurations between MOs with the participation of AOs of nitrogen atoms and oxygens of OH and SO_2 groups; however, the contribution of these configurations to the intensity of the absorption band is very small. Therefore, the presence of SO_2 groups in aminophenol molecules has no effect on the shape of the absorption spectrum. MOs localized on the SO_2 group are more involved in the formation of the short-wavelength range of the spectrum, with energies exceeding 50000 cm^{-1}.

On the whole, analysis of calculation data and their comparison with experimental absorption spectra show satisfactory agreement of calculations and experimental data (Table 3).

Fluorescence spectra and photophysical processes. It appeared that, among all the studied aminophenol, only the AP II and AP VIII compounds possess noticeable fluorescence (Fig. 3). The fluorescence quantum yields of AP II in hexane and acetonitrile are 0.025 and 0.01, respectively, and the fluorescence lifetimes in these solvents are $\tau = 2.5 \times 10^{-10}$ and $\tau = 1 \times 10^{-10}$ s. The wavelength of the fluorescence maximum (λ_{max}) of the solution of AP II in hexane is 320 nm, and, in the solution in acetonitrile, $\lambda_{max} = 309$ nm. Compound AP VIII fluoresces in hexane and acetonitrile with the same quantum yield of $\gamma = 0.007$ and fluorescence lifetime of $\tau = 5 \times 10^{-11}$ s. In both solvents, the fluorescence maximum is observed at $\lambda_{max} = 311$ nm. The fluorescence excitation spectra of AP II and AP VIII coincide in shape and position with the long-wavelength absorption band, and the fluorescence spectra do not depend on the excitation wavelength.

For all the aminophenol derivatives, we calculated the energy schemes of electronically excited states and fluorescence quantum yields. Since the calculated schemes were close to each other, Fig. 4 presents the calculated energy schemes of electronically excited states for one fluorescing (AP II) and one nonfluorescing (AP III) molecule. According to the calculation, for all the derivatives, the radiative decay rate constant is in the range $(2–4) \times 10^7\ s^{-1}$. The internal conversion rate constant does not exceed $6 \times 10^3\ s^{-1}$.

With allowance for experimentally determined fluorescence quantum yields and lifetimes, we estimated the efficiency of nonradiative processes in aminophenol molecules. Neglecting internal conversion processes and assuming that the compounds under study are photostable, we determined the values of the triplet–singlet intersystem crossing rate constant for AP II and AP VIII using the formula $k_{ST} = (1-\gamma)/\gamma \times \tau$. These constants were found to be 2×10^{11} and $3 \times 10^{12}\ s^{-1}$, respectively.

It follows from our calculations that $\pi\pi^*$- and $\pi\sigma^*$ triplet states are energetically close to the $S_1(\pi\pi^*)$ state (Fig. 4). The singlet–triplet intersystem crossing rate constant is known to depend on the energy interval between the interacting singlet and triplet states and on the squared matrix element $\langle|H_{SO}|\rangle$ of the operator of the spin–orbit interaction. The value of this matrix element is primarily determined by the orbital nature of interacting states. A small value of the matrix element between the $\pi\pi^*$ states ($\langle|H_{SO}|\rangle = 0.04\ cm^{-1}$) in aminophenol derivatives yields that the efficiency of the singlet–triplet intersystem crossing is $k_{ST} = 4 \times 10^7–5 \times 10^9\ s^{-1}$. The calculated fluorescence quantum

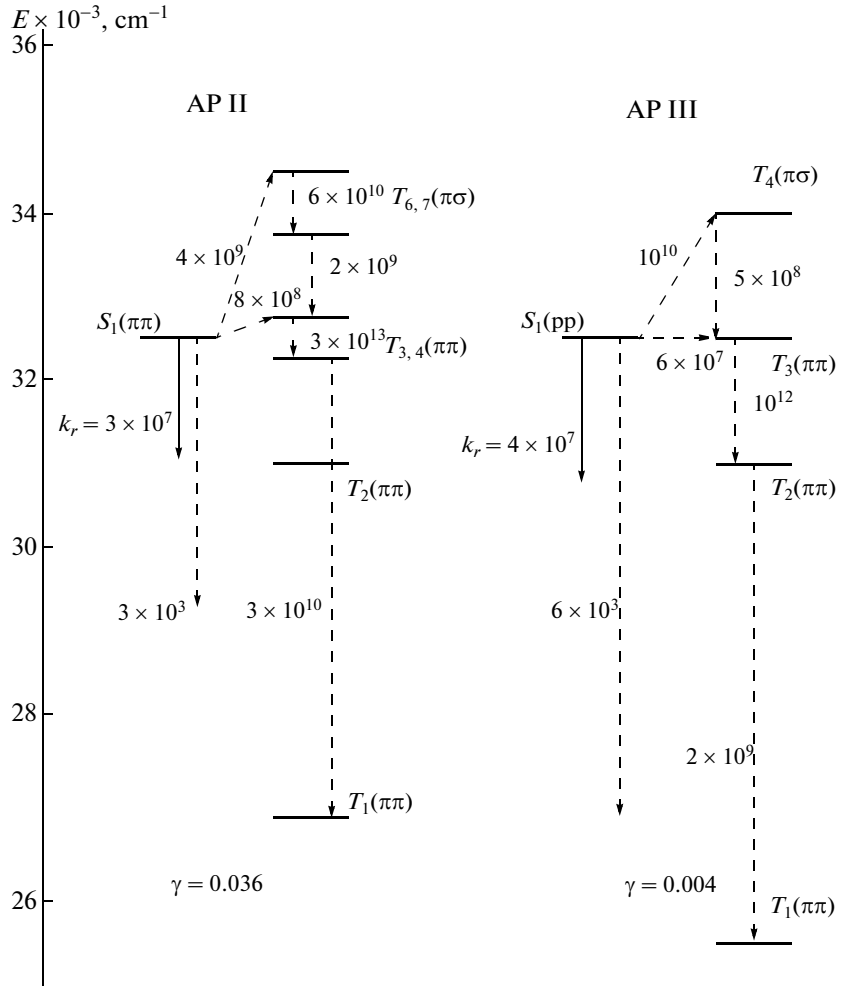

Fig. 4. Energy schemes of electronically excited states and pathways of photophysical processes in AP II and AP III. Figures near arrows indicate rate constants of photophysical processes in reciprocal seconds.

yield is an order of magnitude higher than the experimentally determined values of this parameter.

Triplet states are strongly spin–orbit coupled with the fluorescence state ($\langle|H_{SO}|\rangle \sim 2.00$ cm^{-1}) and lie energetically higher than the $S_1(\pi\pi^*)$ state. Although the energy schemes for compounds AP II and AP III are similar, the energy intervals between the $S_1(\pi\pi^*)$ state and the higher-lying triplet state of the $\pi\sigma^*$ type are different and are 3240 and 1400 cm^{-1}, respectively. When the energy interval is $S_1(\pi\pi^*)$–$T(\pi\sigma^*) \leq 2000$ cm^{-1}, to evaluate pathways of the nonradiative deactivation of the electronic excitation energy, it is expedient to take into account the spin–orbit coupling of the fluorescence state with the $\pi\sigma^*$ triplet state. In this case, taking into account the channel of the energy deactivation $S_1(\pi\pi^*) \rightarrow T(\pi\sigma^*)$ leads to an efficient singlet–triplet intersystem crossing with the rate constant $k_{ST} \sim 10^{10}$ s^{-1}. In this situation, the calculated fluorescence quantum yields become closer the experimental ones. To determine other reasons for the discrepancy between the experimental and calculated fluorescence quantum yields, further investigations are required.

CONCLUSIONS

We studied theoretically and experimentally the electronic structures of anti-HIV active molecules of the class of *o*-aminophenols based on quantum-chemical calculations, IR Fourier-transform spectra, and spectral–luminescent characteristics of these compounds.

We found that the suppression efficiency of HIV infection correlates with the formation of intermolecular bonds of the N–H...O- and O–H...O type involving the participation of OH, NH, and SO_2 groups. We showed that the intensity of bands in the electronic absorption spectra of these compounds is determined by electronic transitions with the participation of the *o*-aminophenol fragment of molecules, with the influence of SO_2 groups being insignificant. We determined

the main channels and mechanisms of photophysical processes in anti-HIV active *o*-aminophenols.

ACKNOWLEDGMENTS

This study was supported by the Russian Foundation for Basic Research (project no. 10-03-90008 Bel_a) and by a Belarusian state program of scientific research (GPNI RB Convergence 3.2.05).

REFERENCES

1. A. A. Klyuchareva, I. V. Petrovich, N. V. Goloborod'ko, and V. V. Komir, *Antiretroviral Therapy for Children: Textbook for Practitioners* (BelMAPO, Minsk, 2004) [in Russian].
2. M. V. Belkov, G. A. Ksendzova, G. I. Polozov, I. V. Skornyakov, V. L. Sorokin, G. B. Tolstorozhev, and O. I. Shadyro, Zh. Prikl. Spektrosk. **74** (5), 577 (2007).
3. E. L. Gasich, V. F. Eremin, G. A. Ksendzova, G. I. Polozov, V. L. Sorokin, and O. I. Shadyro, BY Patent No. 11933 (2009).
4. G. A. Ksendzova, G. I. Polozov, I. V. Skornyakov, V. L. Sorokin, G. B. Tolstorozhev, O. I. Shadyro, and A. A. Yakunin, Opt. Spectrosc. **102** (4), 551 (2007).
5. O. K. Bazyl', V. Ya. Artyukhov, G. V. Maier, T. F. Raichenok, I. V. Skornyakov, G. B. Tolstorozhev, O. I. Shadyro, V. L. Sorokin, and G. A. Ksendzova, Opt. Spectrosc. **107** (4), 564 (2009).
6. M. V. Belkov, G. A. Ksendzova, G. I. Polozov, I. V. Skornyakov, V. L. Sorokin, G. B. Tolstorozhev, and O. I. Shadyro, Zh. Prikl. Spektrosk. **77** (4), 535 (2010).
7. M. V. Belkov, G. A. Ksendzova, I. V. Skornyakov, V. L. Sorokin, G. B. Tolstorozhev, and O. I. Shadyro, Zh. Prikl. Spektrosk. **78** (2), 215 (2011).
8. G. V. Maier, V. Ya. Artyukhov, O. K. Bazyl', T. N. Kopylova, R. T. Kuznetsova, N. R. Rib, and I. V. Sokolova, *Electronically Excited States and Photochemistry of Organic Compounds* (Nauka, Novosibirsk, 1997) [in Russian].
9. http://www.photonics.tsu.ru.
10. T. Scroco and J. Tomasi, Adv. Quant. Chem. **11** (2), 115 (1978).
11. V. Ya. Artyukhov and A. I. Galeeva, Izv. Vyssh. Uchebn. Zaved., No. 11, 96 (1986).
12. http://www.scm.com.
13. O. K. Bazyl', V. Ya. Artyukhov, and G. V. Maier, Izv. Vyssh. Uchebn. Zaved., Fiz. **54** (6), 3 (2011).
14. M. V. Belkov, A. N. Gorbacheva, G. A. Ksendzova, G. I. Polozov, I. V. Skornyakov, V. L. Sorokin, G. B. Tolstorozhev, and O. I. Shadyro, Zh. Prikl. Spektrosk. **77** (3), 340 (2010).

Translated by V. Rogovoi